

BCL6 orchestrates Tfh cell differentiation via multiple distinct mechanisms

Katerina Hatzi,^{1*} J. Philip Nance,^{2*} Mark A. Kroenke,² Marcella Bothwell,^{4,5} Elias K. Haddad,³ Ari Melnick,¹ and Shane Crotty²

¹Division of Hematology and Medical Oncology, Weill Cornell Medical College, Cornell University, New York, NY 10065

²Division of Vaccine Discovery, La Jolla Institute for Allergy and Immunology, La Jolla, CA 92037

³Vaccine and Gene Therapy Institute of Florida, Port St. Lucie, FL 34987

⁴University of California, San Diego Department of Surgery and ⁵Division of Pediatric Otolaryngology, Rady Children's Hospital–San Diego, San Diego, CA 92123

Follicular helper T cells (Tfh cells) are required for T cell help to B cells, and BCL6 is the defining transcription factor of Tfh cells. However, the functions of BCL6 in Tfh cells have largely remained unclear. Here we defined the BCL6 cistrome in primary human germinal center Tfh cells to assess mechanisms of BCL6 regulation of CD4 T cells, comparing and contrasting BCL6 function in T and B cells. BCL6 primarily acts as a repressor in Tfh cells, and BCL6 binding was associated with control of Tfh cell migration and repression of alternative cell fates. Interestingly, although some BCL6-bound genes possessed BCL6 DNA-binding motifs, many BCL6-bound loci were instead characterized by the presence of DNA motifs for AP1 or STAT. AP1 complexes are key positive downstream mediators of TCR signaling and external stimuli. We show that BCL6 can directly bind AP1, and BCL6 depends on AP1 for recruitment to BCL6-binding sites with AP1 motifs, suggesting that BCL6 subverts AP1 activity. These findings reveal that BCL6 has broad and multifaceted effects on Tfh biology and provide insight into how this master regulator mediates distinct cell context-dependent phenotypes.

CORRESPONDENCE

Shane Crotty:
shane@lji.org
OR
Ari Melnick:
amm2014@med.cornell.edu

Abbreviations used: ChIP, chromatin immunoprecipitation; FDR, false discovery rate; GC, germinal center; NES, normalized enrichment score; TES, transcriptional end site; Tfh cell, follicular helper T cell; TSS, transcriptional start site.

Germinal centers (GCs) develop transiently within secondary lymphoid organs upon T cell-dependent antigen exposure and are the source of high-affinity antibody responses. Interactions between activated follicular helper T cells (Tfh cells) and B cells are required for the formation and function of GCs (Crotty, 2014). Intriguingly, the BCL6 transcriptional repressor protein is essential for the formation of both Tfh cells and GC B cells; BCL6-deficient mice fail to develop GCs as the result of cell-autonomous effects in each of these cell types (Cattoretti et al., 1995; Dent et al., 1997; Johnston et al., 2009; Nurieva et al., 2009; Yu et al., 2009). The requirement of BCL6 in both GC B and CD4 T cells has been puzzling because these cells have very different specialized functions and hence there were no obvious parallels pointing to similar BCL6-regulated transcriptional programs in these cell types. GC B cells proliferate rapidly and tolerate genomic damage and stress associated with somatic hypermutation. Tfh cells are a specialized subset of CD4⁺ T cells that migrate into

B cell follicles to provide help to GC B cells via costimulatory receptors and secretion of cytokines (Crotty, 2015).

To date, few genes have been demonstrated to be directly regulated by BCL6 in Tfh cells. For example, BCL6 was shown to repress the *PRDM1* locus in both Tfh and GC B cells (Tunayaplin et al., 2004; Johnston et al., 2009). BCL6 repression of *PRDM1* prevents differentiation of both cell types and represents a commonality between B and T cells (Shaffer et al., 2000). Most notably, current studies have only addressed BCL6 regulation of rare single loci. Moreover, it is currently not known whether BCL6 acts predominantly as a transcriptional activator or repressor in Tfh cells. Hence, the genome-wide BCL6 transcriptional network and the BCL6 mechanisms of action in GC Tfh cells remain unknown.

© 2015 Hatzi et al. This article is distributed under the terms of an Attribution-Noncommercial-Share Alike-No Mirror Sites license for the first six months after the publication date (see <http://www.rupress.org/terms>). After six months it is available under a Creative Commons License (Attribution-Noncommercial-Share Alike 3.0 Unported license, as described at <http://creativecommons.org/licenses/by-nc-sa/3.0/>).

*K. Hatzi and J.P. Nance contributed equally to this paper.

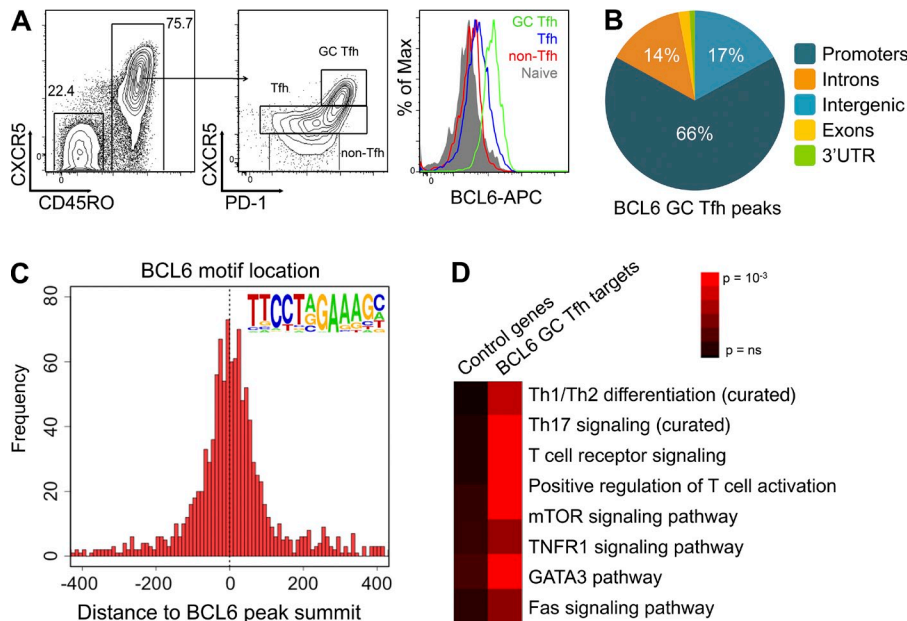


Figure 1. BCL6 binds thousands of Tfh genes involved in T cell-related biological networks. (A) Cell sorting strategy for the isolation of GC Tfh cells and BCL6 staining of individual populations. (B) Pie chart of the genome-wide distribution of BCL6 Tfh peaks based on RefSeq. Peaks occurring within ± 2 kb of the TSS and TES were considered promoter and 3'UTR peaks, respectively. (C) Frequency of BCL6 motifs present in BCL6 peaks localized relative to the BCL6 peak summit. (D) Pathway analysis of genes associated with BCL6 peaks using the GO and KEGG databases and curated T cell datasets. Color key indicates p-value enrichment. Data are from two experiments, comprising primary Tfh cells from three human donors.

To better understand the mechanisms by which BCL6 directly regulates Tfh cells, we performed a comprehensive study of BCL6 genomic localization and transcriptional effects in primary human Tfh cells. Integration of these and other data revealed a Tfh-specific BCL6 cis-regulatory genome landscape that controls critical T cell-specific pathways, including cell migration and alternative T cell fates. Moreover, BCL6 genomic distribution exhibited distinct and characteristic features. Among these was the surprisingly prominent overlap with the major activating complex AP1, suggestive of a key counter-regulatory relation between these transcription factors in T cells. Our results reveal that BCL6 is a multifaceted regulator of the Tfh lineage, using multiple mechanisms to control Tfh cell biology.

RESULTS

The GC Tfh BCL6 cistrome

BCL6 is the central regulator of GC Tfh cell differentiation; however, the genome-wide target gene network that BCL6 regulates in these cells remains unknown. To determine the distribution of BCL6-bound cis-regulatory regions in GC Tfh cells (the BCL6 cistrome), we performed BCL6 chromatin immunoprecipitation (ChIP) sequencing (ChIP-seq) of primary GC Tfh cells (CXCR5^{hi} PD1^{hi} CD45RO⁺ CD4 T cells) freshly isolated from human tonsils (Fig. 1 A). Tonsils are a lymphoid organ rich in GCs and GC Tfh cells. Using stringent sequence abundance peak detection thresholds and the overlap of two highly correlated ($r = 0.75$) independent biological BCL6 ChIP-seq replicates, we identified 8,523 GC Tfh genomic loci with significant BCL6 binding. These ChIP-seq replicates were performed using chromatin from three GC Tfh isolations to minimize potential binding biases between individual tonsil donors. The BCL6-binding sites were predominantly localized to GC Tfh promoters (66%),

whereas intergenic (17%) and intronic regions (14%) were also substantially represented (Fig. 1 B). To determine whether the BCL6-binding motif was enriched among these BCL6-binding sites, we performed an unsupervised de novo DNA motif analysis (Heinz et al., 2010). The BCL6 motif was significantly overrepresented among BCL6 peaks from GC Tfh cells ($P = 10^{-221}$). Moreover, the BCL6 peak summit (the region of each peak with highest enrichment of BCL6-bound DNA) strongly clustered around the BCL6 canonical DNA-binding motif, further validating this BCL6 GC Tfh ChIP-seq dataset (Fig. 1 C). To gain insight into the biological pathways targeted by BCL6 in GC Tfh cells, we identified the genes associated with BCL6-binding sites in these cells and their biological functions (Fig. 1 D). Genes encoding components of Th1 cell differentiation (Fig. 2 A), Th17 cell differentiation (Fig. 2 B), Th2 cell differentiation (Fig. 2 C), T reg cell differentiation (Fig. 2 D), and migration-associated genes (Fig. 2 E) were highly enriched for BCL6 targets in GC Tfh cells. These results suggest that BCL6 facilitates Tfh cell migration and differentiation and additionally “locks in” the GC Tfh phenotype by antagonizing alternative T cell effector programs. Although it was previously found that BCL6 could bind a few genes associated with alternative cell fates, here we show that BCL6 binds thousands of genes in GC Tfh cells, and those bound loci are highly enriched for genes involved in T cell differentiation fates. Furthermore, the whole genome BCL6 ChIP-seq analysis indicates that BCL6 has multiple redundant ways to inhibit each of the alternative effector T cell differentiation pathways. This helps explain previous observations that BCL6 could impact GATA3-associated Th2 functions and ROR γ t-associated Th17 functions without evidence of binding GATA3 or RORC directly (Kusam et al., 2003; Nurieva et al., 2009). Of note, we saw no evidence of BCL6 binding to the RORC gene, unlike Yu et al. (2009)

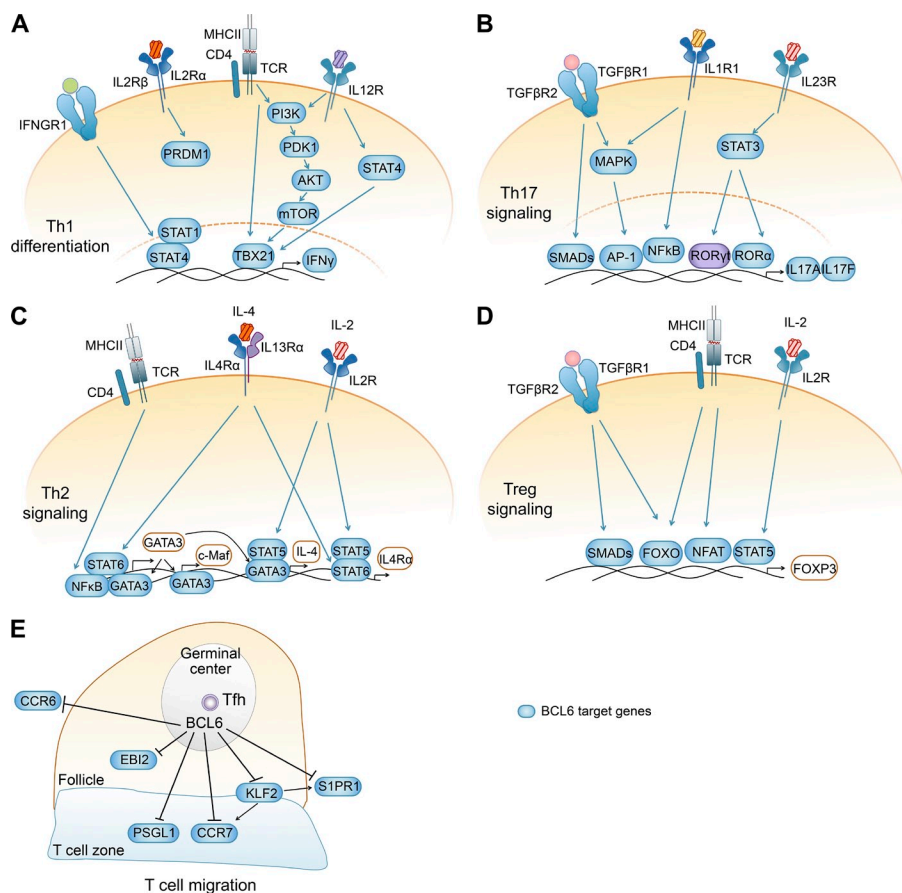


Figure 2. BCL6 targets Tfh genes mainly involved in T cell signaling, differentiation, and migration pathways to drive the GC Tfh phenotype. (A–E) Graphical representation of BCL6 targeted pathway components involved in T cell receptor signaling (A), Th17 cell differentiation (B), Th2 cell differentiation (C), T reg cell signaling (D), and T cell migration (E). Proteins encoded by genes bound by BCL6 are shown in blue. Data are from two experiments, comprising primary Tfh cells from three human donors.

but in agreement with Nurieva et al. (2009); in contrast, we observed very robust BCL6 binding to *RORA* (see below), the other ROR family member that controls Th17 cell differentiation (Yang et al., 2008). A prominent BCL6 peak was also present at the *IL17A/F* enhancer locus (see below). Although BCL6 bound a network of T reg genes, we observed no binding to the *FOXP3* locus. BCL6 ChIP-seq also revealed direct BCL6 binding to the *FOXO1* promoter. *FOXO1* inhibits Tfh cell differentiation (Xiao et al., 2014; Stone et al., 2015).

A defining feature of Tfh cells is their colocalization with B cells in follicles and GCs. The ChIP-seq data suggest that BCL6 regulation of T cell migration is a major mechanism by which BCL6 controls Tfh biology. Non-Tfh effector cells exit LNs in an *S1PR1*-dependent manner and migrate to sites of inflammation and infection. In GC Tfh cells, BCL6 bound the *S1PR1* gene and a large *S1PR1* proximal enhancer. BCL6 also bound the *KLF2* promoter. *KLF2* is a positive regulator of *S1PR1* expression (Carlson et al., 2006), and repression of *KLF2* is necessary for Tfh differentiation (Lee et al., 2015; Weber et al., 2015). Tfh cells localize to B cell follicles because they express *CXCR5*, but also because they down-regulate *CCR7* and *PSGL1* (*SELPLG*), which cause localization to the T cell zone. Both *SELPLG* and *CCR7* are highly enriched for BCL6 binding in GC Tfh cells (see below). An additional chemotactic receptor, *EBI2* (*GPR183*), is important for localization of B cells to follicles but specifically outside of

GCs (Gatto et al., 2009; Pereira et al., 2009) and is repressed by BCL6 in GC B cells (Shaffer et al., 2000; Huang et al., 2014). *EBI2* is also likely important in Tfh localization, as *EBI2* expression is specifically reduced in GC Tfh cells and *GPR183* is bound by BCL6 (Fig. 2 E). All of the migration-associated genes shown in Fig. 2 E are differentially expressed in GC Tfh cells (Rasheed et al., 2006; Ma et al., 2009; Locci et al., 2013). Combined with the recognition that BCL6 expression results in up-regulation of *CXCR5*, *CXCR4*, and *SAP* in human CD4T cells (whereas up-regulation of *CXCR5* in vitro on mouse CD4T cells does not depend on BCL6 (Liu et al., 2014), but most *CXCR5* expression in vivo is BCL6 dependent (Poholek et al., 2010; Choi et al., 2011), these data indicate that BCL6 may participate in the control of most aspects of GC Tfh migration.

BCL6 directly represses a broad network of promoters

To understand the cis-regulatory landscape of GC Tfh cells, we next performed ChIP-seq for the epigenetic marks H3K4me1, H3K4me3, and H3K27ac, which are histone modifications that mark promoters and enhancer regions. These ChIP-seq experiments were again performed using primary human GC Tfh cells, directly ex vivo. Ranking of GC Tfh gene promoters by decreasing BCL6 binding density within ± 5 kb of known transcriptional start sites (TSSs) showed that the bulk of BCL6 binding in GC Tfh cells occurs in promoters enriched

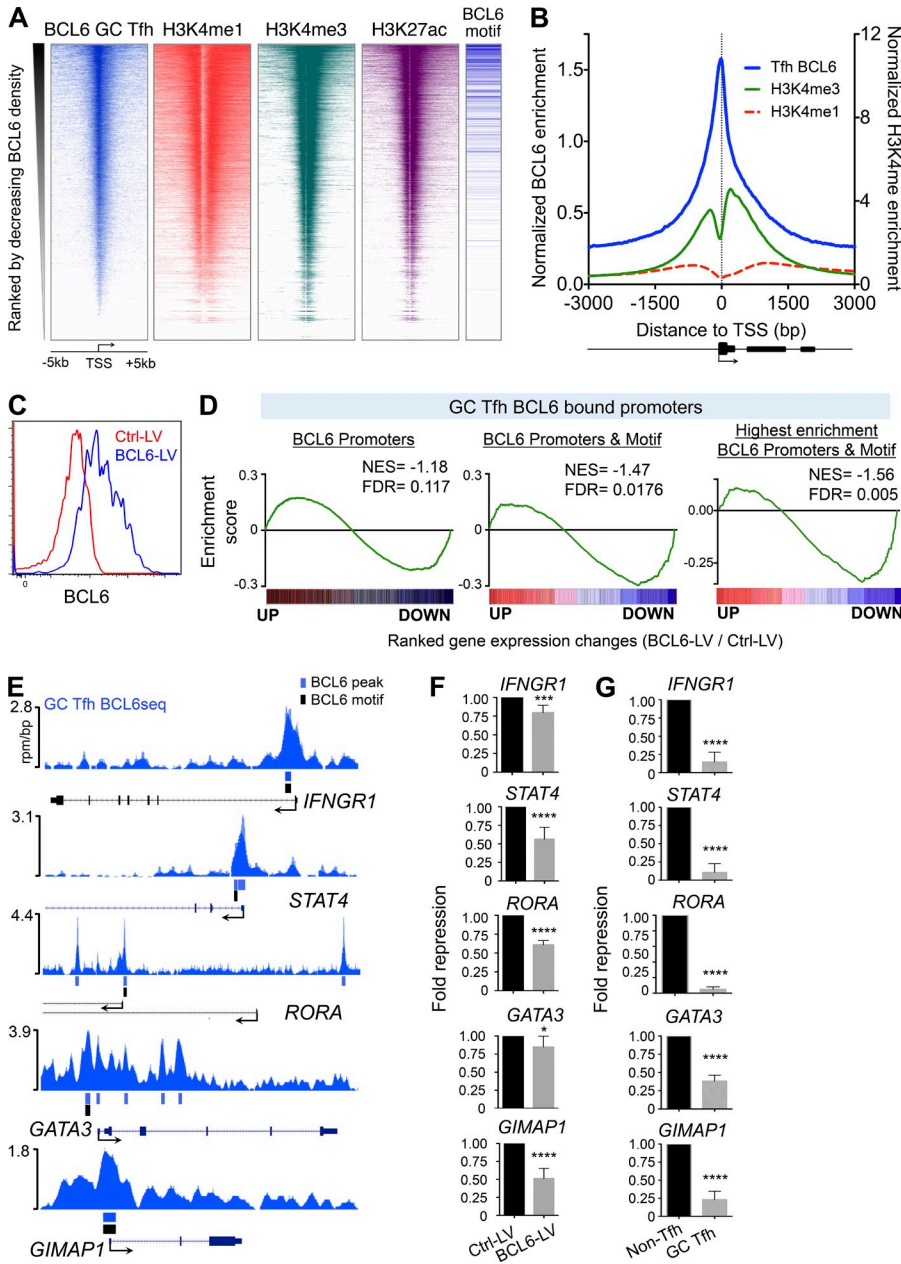


Figure 3. BCL6 most potently represses promoters where it binds to its cognate DNA motif. (A) Normalized read density profiles of all gene promoters in Tfh cells ranked from high to low BCL6 read density for GC Tfh BCL6, H3K4me1, H3K4me3, and H3K27ac ChIP-seq. Promoters with BCL6 peaks containing BCL6 motifs are marked blue. (B) Mean normalized read density profiles of H3K4 methylation marks and BCL6 density surrounding the TSSs in GC Tfh cells. Density values were normalized to the total number of reads. (C) BCL6 flow cytometry staining of T cells transduced with BCL6-LV or control vector (Ctrl-LV). (D) GSEA analysis based on global gene expression changes after BCL6 lentiviral induction in CD4 T cells versus control lentivirus. Up and down indicate the relative gene up- or down-regulation after BCL6 expression. The gene sets used were all Tfh genes with BCL6 promoter binding (left), Tfh genes with BCL6 promoter peaks containing the BCL6 motif (middle), and Tfh genes with high enrichment BCL6 promoter peaks (top 25%) that contained BCL6 motifs (right). FDR is based on 1,000 permutations. (E) Read density tracks of BCL6 ChIP-seq enrichment in selected GC Tfh cell promoters. BCL6 peaks are indicated by a blue box, whereas BCL6 motifs are indicated by a black box (rpm, reads per million). ChIP-seq data are from two experiments, comprising primary CD4 T cells from three human donors. (F) Microarray comparison of BCL6 target gene expression levels for *IFNGR1*, *STAT4*, *RORA*, *GATA3*, and *GIMAP1* in BCL6-LV+ CD4 T cells relative to CD4 T cells transduced with control vector. Data are from six independent donors. (G) Comparison of BCL6 target gene expression levels in CXCR5^{hi} (GC Tfh) versus CXCR5⁻ cells (non-Tfh) calculated by qPCR. Data are from four independent donors and are representative of two independent experiments. Fold changes were normalized to *GAPDH* and are shown relative to non-Tfh. (F and G) Error bars indicate SEM. *, P < 0.05; ***, P < 0.001; ****, P < 0.0001.

in H3K4me1, H3K4me3, and H3K27ac, which is a signature characteristic of actively transcribed genes (Fig. 3 A). To assess the link between BCL6 binding and nucleosome positioning at promoters, we determined the mean H3K4me1, H3K4me3, and BCL6 enrichment profile in these regions. This promoter chromatin profile indicates that BCL6, on average, occupies the nucleosome-free region just upstream of the TSS (Fig. 3 B). Enrichment of BCL6 binding to regions with active chromatin marks was unexpected, as BCL6 is known as a repressor, and it is not known to activate gene expression. Hence, its binding to genes with active chromatin marks may signify that BCL6 predominantly represses or dampens the expression of transcriptionally activated, or transcriptionally poised, genes in

Tfh cells. Alternatively, BCL6 may be acting as a transcriptional activator in GC Tfh cells.

To explore these different possibilities, we performed experimental perturbations of BCL6 expression. Purified primary naive human CD4 T cells were transduced with a BCL6-expressing lentiviral vector (BCL6-LV; Fig. 3 C), and gene expression profiling was performed. Gene expression analysis at day 5 after transduction revealed that 457 genes with BCL6-bound promoters in GC Tfh cells were repressed in CD4 cells upon expression of BCL6 (>1.25-fold, false discovery rate [FDR] < 0.05). There was a trend for promoters with BCL6 peaks to be repressed after induction of BCL6 in T cells (normalized enrichment score [NES] = -1.18,

FDR = 0.117; Fig. 3 D). Furthermore, promoters with BCL6 peaks that contain a BCL6 DNA motif were significantly enriched among genes repressed upon expression of BCL6 (NES = -1.47, FDR = 0.0176). In GC Tfh cells, promoters containing a BCL6 DNA-binding motif were enriched among the most prominent BCL6 peaks (Fig. 3 A). Genes associated with the largest BCL6 promoter peaks and containing BCL6 DNA motifs were especially highly enriched among those genes repressed by BCL6 (FDR = 0.005, NES = -1.56; Fig. 3 D). These results are consistent with BCL6 acting primarily as a direct transcriptional repressor in GC Tfh cells. *KLF2* expression was the most strongly repressed gene transcript overall. BCL6 target promoters with BCL6-binding sites included the genes *IFNGR1*, *STAT4*, *GATA3*, and *RORA* (Fig. 3 E), which play key roles in differentiation of Th1, Th2, and Th17 cells. BCL6 also bound a BCL6 DNA-binding motif in the promoter of *GIMAP1*, a regulator of T cell proliferation. We observed a significant reduction of *RORA*, *GIMAP1*, and *STAT4* expression in BCL6-LV⁺ CD4 T cells ($P < 0.001$) and a moderate reduction of *IFNGR1* and *GATA3* (Fig. 3 F). Furthermore, quantitative PCR (qPCR) analysis of GC Tfh cells from different donors revealed reduced transcript abundance of each of these genes in GC Tfh cells compared with naive T cells (Fig. 3 G).

BCL6 represses different subsets of promoters in Tfh cells and GC B cells

GC B cells are phenotypically very different compared with Tfh cells. Given that BCL6 is a lineage-defining transcription factor of both cell types, it is logical to posit that it regulates different gene sets in each case. Interestingly, comparison of BCL6-binding sites using ChIP-seq from human primary GC B cells (Huang et al., 2013) reveals that approximately half of GC Tfh BCL6-binding sites (4,321 peaks) are shared between GC B and GC Tfh cells (Fig. 4 A). Nonetheless, a large fraction of BCL6 peaks were specific to each cell type. 49% of GC Tfh ($n = 4,202$) and 66% of GC B cell BCL6 peaks ($n = 10,133$) were unique to B and T cells, respectively (Fig. 4 A). These GC B-only and GC Tfh-only BCL6 peaks had low enrichment of BCL6 binding in the other cell type (Fig. 4, B and C). This suggests that BCL6 regulates both common and cell context-dependent functions. Notably, the vast majority of common GC Tfh B cell BCL6 peaks were localized to promoter regions (76%; TSS \pm 2 kb; Fig. 4 D). The *BCL6* and *PRDM1* promoters were among those with robust BCL6 promoter binding in both GC Tfh and GC B cells (Fig. 4 E). A large fraction of the GC Tfh-only and GC B cell-only BCL6 peaks were in intergenic and intronic sites, suggestive of cell type-specific enhancers (Fig. 4, F and H). For example, several intergenic GC B cell-only BCL6-binding sites were present near the *SYK* and *MSH6* loci in GC B cells but were absent in GC Tfh cells (Fig. 4 G). On the contrary, BCL6 bound to intergenic sites upstream of *IL21* and *PLCG1* loci in GC Tfh cells but was not enriched at the corresponding locations in GC B cells (Fig. 4 G). Another interesting example is *SELPLG*, a regulator of Tfh migration, for which

there were different BCL6-bound loci in GC Tfh and GC B cells (Fig. 4 J). These results were validated by qChIP experiments using chromatin from GC B and Tfh cell isolations from several independent donors (Fig. 4 K).

Because most of the cell context-dependent BCL6 targets occur outside gene promoters, we examined the chromatin architecture surrounding these sites. We found that the chromatin marks H3K4me1 and H3K27ac, which are associated with enhancers, were selectively enriched in the GC B-only and GC Tfh-only BCL6 loci in B and T cells, respectively, but were largely absent in the opposite cell type (Fig. 5). On the contrary, both of these histone marks were enriched in the smaller subset of common T-B peaks both in T and in B cells. This result highlights that the role of BCL6 is associated with unique cell context-specific chromatin landscapes.

Given that BCL6 binding does not necessarily equate to transcriptional regulation, we wanted to know whether these promoters were also regulated by BCL6 in both B and Tfh cells. 457 BCL6 Tfh promoter target genes were significantly repressed by BCL6 induction in CD4 T cells, as noted earlier (Fig. 3 D). We also observed that 518 BCL6 promoter target genes were significantly up-regulated after siRNA-mediated BCL6 knockdown in GC-derived B cells (>1.5-fold, FDR < 0.05). We observed that despite the extensive overlap (70%) of BCL6 binding at B and Tfh cell promoters, only 72 genes (16%) had evidence of repression by BCL6 in both cell types. BCL6 repressed *PRDM1*, *S1PR4*, *CD69*, *LPP*, *FAIM3*, *PTEN*, *CASP8*, *FOXO3*, and *CDKN1B* in both GC B and Tfh cells, among other genes. The common module may be required for migration of these cells into the follicle after GC chemokine gradients or may reflect common signaling cues from the GC microenvironment. Several common components of the B and T cell receptor pathway were also targeted by BCL6 in both cells. Overall, although there are limitations to this analysis, these data indicate that many bound promoters are only repressed by BCL6 in either GC Tfh or GC B cells. BCL6 represses gene expression via recruitment of corepressors (Hatzl and Melnick, 2014), and thus these data imply a possible important role for differential expression or utilization of BCL6 corepressors in Tfh cells versus GC B cells. Alternatively, pioneering complexes and distinct chromatin nuclear topology might regulate the accessibility of specific loci to BCL6 complexes.

BCL6 targets a network of GC Tfh cell-specific enhancers

34% of BCL6-binding sites in GC Tfh were in introns or intergenic loci, indicating possible association with enhancers. Enhancers can be defined as discrete promoter-distal (upstream or downstream) genomic regions enriched in H3K4me1 but depleted of H3K4me3. The enhancer landscape (histone modifications) of human Tfh cells is distinct from non-Tfh cells (Weinstein et al., 2014). To ascertain whether nonpromoter BCL6-binding sites in GC Tfh cells corresponded to enhancers, we determined the overlap of BCL6 GC Tfh peaks with regions significantly enriched in H3K4me1 and lacking H3K4me3. From this analysis, 1,016 BCL6-binding sites mapped

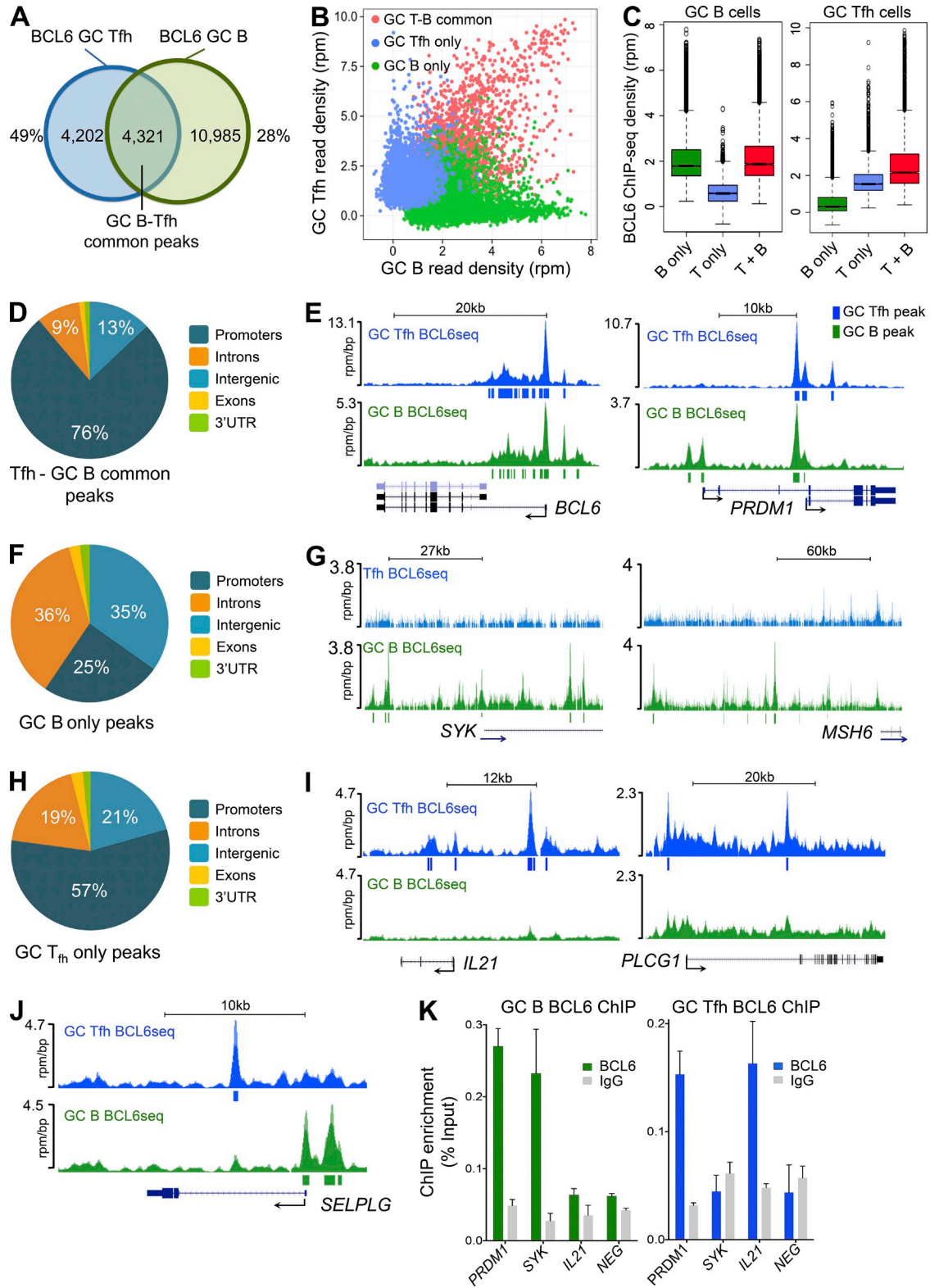


Figure 4. BCL6 binding and gene regulation in Tfh cells differs compared with GC B cells with distinct pattern mainly outside promoters. (A) Overlap of BCL6-binding sites in Tfh (blue) and GC B cells (green). (B) Normalized BCL6 ChIP-seq read densities plotted for Tfh cells (y axis) versus B cells (x axis) for each peak corresponding to peaks common to Tfh and B cells, Tfh-only peaks, and B cell-only peaks. Density values were normalized to the total number of reads (rpm, reads per million). (C) Boxplots comparing BCL6 Tfh and GC B BCL6 ChIP-seq read densities for B cell-only peaks, Tfh-only peaks, and peaks common to Tfh and B cells. Density values were normalized to the total number of reads. (B and C) Input chromatin density was subtracted

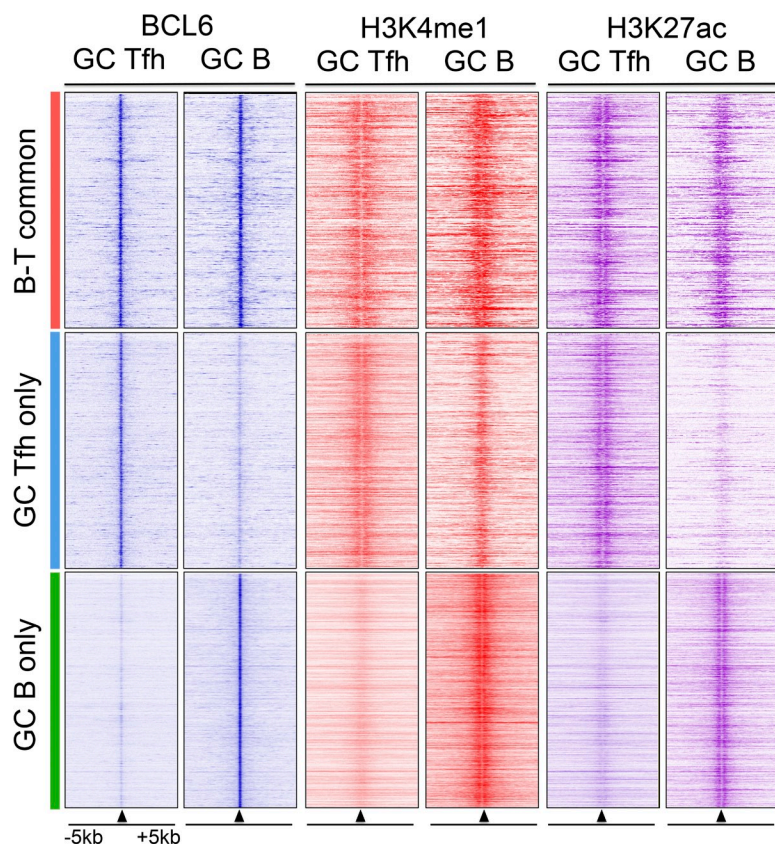


Figure 5. Comparison of specialized BCL6 GC Tfh and GC B cell targeted chromatin landscape. Heat maps of read density profiles of BCL6, H3K4me1, and H3K27ac ChIP-seq in GC B and Tfh cells surrounding BCL6 peaks outside promoters. Maps were centered at the BCL6 peak summit and were separated in peaks common to GC B and T cells, GC Tfh-only peaks, and GC B-only peaks. T cell ChIP-seq data are from two experiments, comprising primary CD4 T cells from three human donors. Values were normalized to the total number of reads.

to GC Tfh enhancer elements. The mean pattern of BCL6 and H3K4me1 enrichment at these sites suggests that BCL6 binds between nucleosomes and directly accesses DNA containing its cognate motif localized there (Fig. 6 A). Many enhancers with critical gene regulatory functions are conserved among species. We found that the conservation index of BCL6-bound enhancers was highly significantly increased compared with random loci ($P < 0.001$; Fig. 6 B), suggesting that these are functionally relevant binding sites. Enhancers are known to mediate cell context-specific gene regulation. Hence, we next asked whether the enhancers occupied by BCL6 in Tfh cells are also bound by BCL6 in GC B cells. The majority of GC Tfh BCL6-bound enhancers (743/1,016; 73%) were specific to Tfh cells as they were not bound by BCL6 in GC B cells. These loci were not marked by H3K4me1 or H3K27ac in GC B cells, indicating that these

loci have a gene regulatory role in Tfh cells but not in B cells (Fig. 6 C). These findings suggest that BCL6 mediates distinct functions in GC Tfh versus GC B cells by targeting cell type-specific enhancers.

Enhancers are defined as being in active or poised configuration based on the presence or absence of H3K27ac. The majority of BCL6-bound GC Tfh enhancers (76%, 757) were depleted of H3K27ac, reflecting an inactive (poised) conformation (Fig. 6 D), suggesting a putative role of BCL6 in enhancer silencing in Tfh cells. To test how BCL6 enhancer regulation may affect gene expression, we performed GSEA analysis of the gene set of the poised enhancer proximal genes, assessing ranked gene expression changes after induction of BCL6 in CD4 T cells using BCL6-LV⁺ or control lentivirus. We found a highly significant enrichment in repression among total genes associated with BCL6-bound poised enhancers in

from each measurement. (D) Pie chart of the genome-wide distribution of BCL6 peaks common in GC B cells and GC Tfh cells based on RefSeq. Peaks occurring within ± 2 kb of the TSS and TES were considered promoter and 3'UTR peaks, respectively. (E) BCL6 density tracks of *BCL6* and *PRDM1* loci that were commonly bound in GC Tfh and GC B cells. Read densities are shown in blue for GC Tfh BCL6 ChIP-seq and green for GC B BCL6 ChIP-seq. (F) Pie chart of the genome-wide distribution of GC B-only BCL6 peaks. (G) BCL6 density tracks of *SYK* and *MSH6* that were bound by BCL6 in GC B cells but not in GC Tfh cells. (H) Pie chart of the genome-wide distribution of Tfh-only BCL6 peaks. (I) BCL6 density tracks the *IL21* and *PLCG1* loci that were bound by BCL6 in GC Tfh cells but not in GC B cells. (J) Tfh and GCB BCL6 read density on the *SELPLG* locus where BCL6 binds at different sites. ChIP-seq data are from two experiments, comprising primary CD4 T cells from three human donors. (K) qChIP experiments confirm BCL6 is selectively enriched at the *SYK* and *IL21* loci in GC B and GC Tfh cells, respectively. BCL6 binds the *PRDM1* promoter in both B and T cells. Nonspecific IgG antibody was used as a negative immunoprecipitation control. Data for cells from three separate donors are shown, representative of two independent experiments. Values are shown as percentage of input chromatin. The BCL6 intron 9 served as a negative control locus. Error bars indicate SEM.

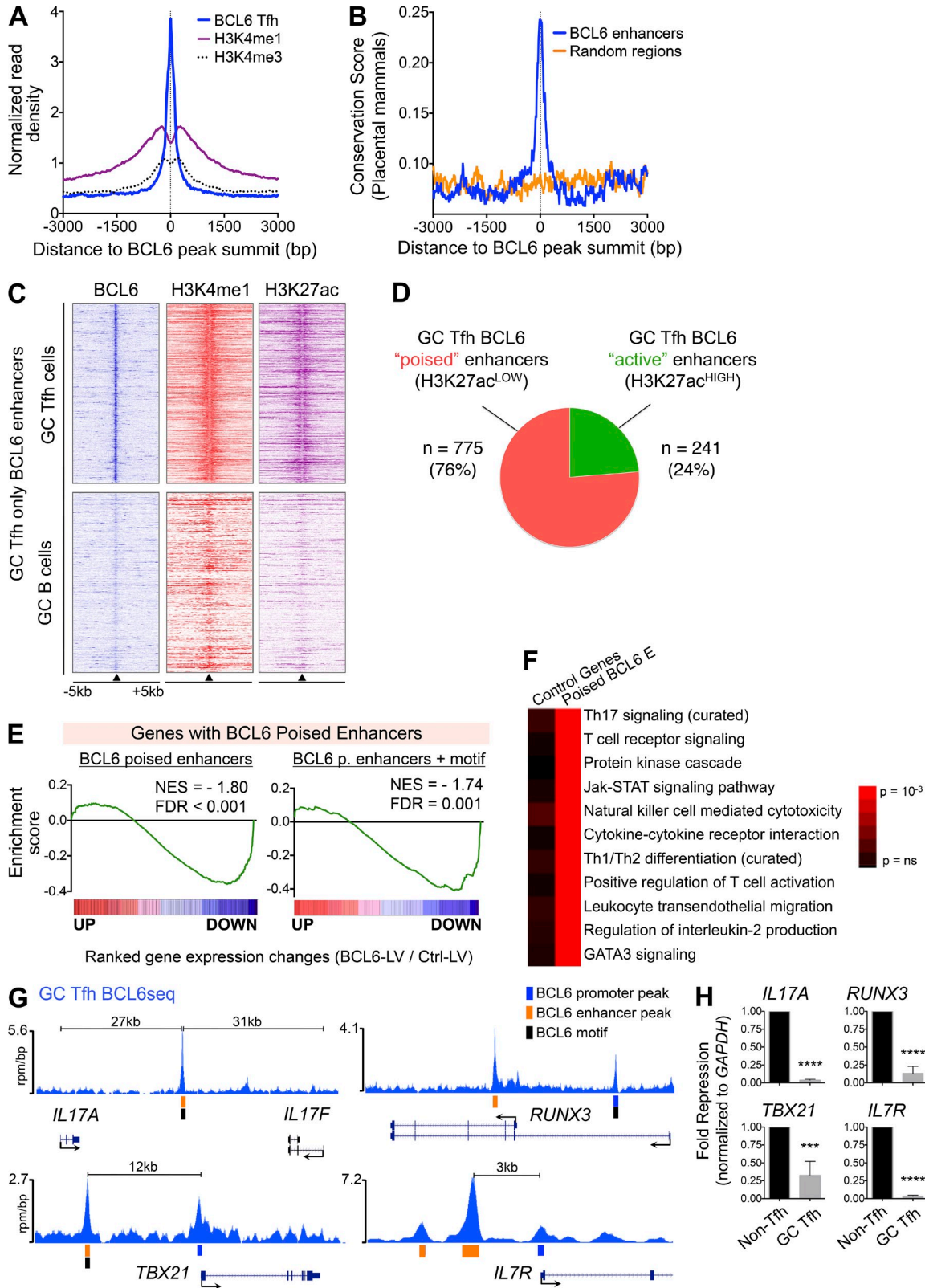


Figure 6. BCL6 targets T cell-specific enhancers associated with transcriptional repression and a poised chromatin configuration. (A) BCL6 and H3K4me1 ChIP-seq density profiles derived from GC Tfh cells (blue). Enrichment represents the mean normalized read density in Tfh-only BCL6-bound enhancers. (B) Mean conservation score (placental mammal phastCons) of BCL6-bound enhancers relative to the BCL6 peak summit. Random regions were used as a control. (C) Heat maps representing BCL6, H3K4me1, and H3K27ac normalized read density in GC Tfh-only BCL6 enhancers in GC Tfh

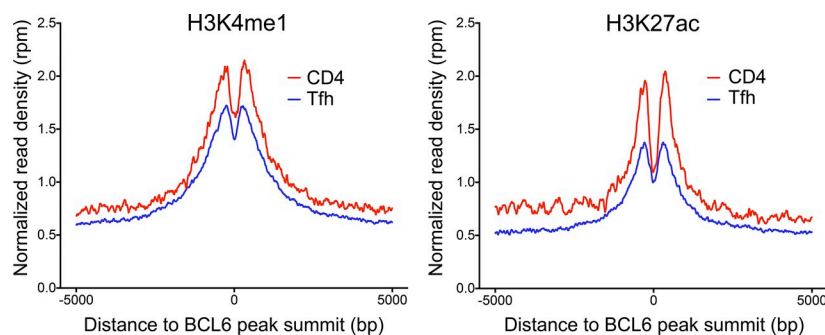


Figure 7. Enhancer chromatin profiles during Tfh cell differentiation. Mean ChIP-seq density profiles of the H3K4me1 and H3K27ac chromatin marks in CD4 T cells and GC Tfh cells surrounding BCL6 peaks. Plots were centered at the BCL6 peak summit and represent poised Tfh enhancers bound by BCL6. ChIP-seq data are from two experiments, comprising primary CD4 T cells from three human donors. Values were normalized to the total number of reads.

GC Tfh cells (NES = -1.80 , FDR < 0.001 ; Fig. 6 E). Enhancers containing BCL6 DNA-binding motif genes bound by BCL6 (linked to 170 genes) were equally enriched for repression in BCL6-expressing CD4 T cells (NES = -1.74 , FDR = 0.001 ; Fig. 6 E). To understand what type of transcriptional programs BCL6 regulates through enhancer binding, we performed pathway analysis on the set of genes linked to poised BCL6 GC Tfh enhancers. We found that these genes were significantly enriched in biological pathways relevant to T cells biology, including T cell activation, Th17 biology, Th1/Th2 cell differentiation, T cell receptor signaling, protein kinase cascade, and Jak-Stat signaling (Fig. 6 F). T cell-specific gene enhancers containing a BCL6 motif directly bound by BCL6 in GC Tfh cells included *TBX21*, *RUNX3*, *IL7R*, and the *IL17A/F* enhancer (Fig. 6 G). Each of these genes is repressed in human GC Tfh cells (Fig. 6 H). The *IL17A/F* enhancer, in particular, is known to be a critical regulator of Th17 function (Yang et al., 2011). The reduction in H3K27 acetylation at BCL6-bound enhancers suggests that BCL6 may promote histone deacetylation at these sites to antagonize p300 histone acetyltransferase activity. This could occur via BCL6 recruitment of histone deacetylase-containing complexes such as SMRT/NCOR or NuRD (Hatzi and Melnick, 2014). To further investigate this finding, we asked how the chromatin surrounding the BCL6-poised enhancers changes during T cell differentiation. Therefore, we generated and compared chromatin profiles of the enhancer histone marks H3K4me1 and H3K27ac in naive CD4 T cells (CD4⁺CD25⁻CD45RA⁺; Andersson et al., 2014) and GC Tfh cells (Fig. 7). Enrichment of both marks decreased in Tfh cells compared with CD4 naive T cells. This finding supports a potential role of BCL6 in decommissioning T cell enhancers during differentiation. Collectively, these data reveal that

BCL6 mediates its actions in GC Tfh cells by repressing networks of gene promoters and enhancers.

Extensive AP1 and BCL6 interactions at promoters and enhancers in GC Tfh cells

The canonical function of BCL6 involves repression of genes by directly binding to cis-regulatory elements containing a BCL6 DNA-binding motif (Figs. 3 E and 6 G). Strikingly, the vast majority of BCL6-bound loci in GC Tfh cells, 88%, lacked a BCL6 DNA-binding motif. We considered that BCL6 may be primarily recruited to DNA by other transcription factors in GC Tfh cells. To test this hypothesis, we first performed an unbiased DNA motif discovery analysis. The BCL6 DNA motif was the top motif observed ($P = 10^{-221}$, observed in 1,043 peaks, 12%; motif shown in Fig. 1 C; TTCCTAGAAAGC), but in addition, AP1 ($P = 10^{-112}$; Fig. 8 A) and STAT transcription factor motifs ($P = 10^{-80}$; Fig. 8 A) were also highly ranked and highly enriched among BCL6-bound peaks in GC Tfh cells. To ascertain whether these BCL6-binding sites were bona fide STAT and AP1 targets in T cells, we cross-referenced the peaks to published ChIP-seq datasets from activated CD4 T cells. This analysis indicated that a majority of BCL6-binding peaks containing STAT- or AP1-binding motifs are indeed bound by STAT3 and AP1 family proteins (Fig. 8 B). Promoters or enhancers with consensus STAT motifs (TTC[N₁₋₃]GAA) within BCL6 peaks were significantly associated with repression by BCL6 in BCL6-LV⁺ T cells (FDR = 0.003 and FDR < 0.001 ; Fig. 8 C). STAT proteins mold the enhancer landscape of helper T cells (Vahedi et al., 2012), and it is known that STAT consensus motif sequences can often be observed embedded in BCL6 DNA motifs. Accumulating evidence suggests that in B cells and macrophages BCL6 may antagonize STAT signaling (Dent et al., 1997;

cells versus GC B cells. (D) Pie chart representing the proportion of BCL6 GC Tfh enhancer peaks (H3K4me1⁺) that are enriched (green) or depleted (red) in H3K27ac, which positively correlates with enhancer activity. (E) GSEA analysis of genes associated with “poised” BCL6-bound Tfh enhancers and “poised” BCL6-bound Tfh enhancers that also contained the cognate BCL6 motif. GSEA was performed using gene expression changes induced by BCL6 transduction in CD4 T cells. Up and down indicate the relative gene up- or down-regulation after BCL6 expression. 1,000 permutations were used. (F) Pathway analysis of genes linked to “poised” BCL6 Tfh enhancers using PAGE. Color key indicates enrichment p-values. (G) Read density tracks of BCL6 ChIP-seq enrichment in selected GC Tfh cell enhancers. BCL6 peaks are indicated by a blue box, whereas BCL6 motifs are indicated by a black box. T cell ChIP-seq data are from two experiments, comprising primary CD4 T cells from three human donors. (H) Comparison of BCL6 target gene expression levels in CXCR5⁺ (GC Tfh) versus CXCR5⁻ cells (non-Tfh) calculated by qPCR. Data are from four independent donors and are representative of two independent experiments. Fold changes were normalized to GAPDH and are shown relative to non-Tfh. Error bars indicate SEM. ***, $P < 0.001$; ****, $P < 0.0001$.

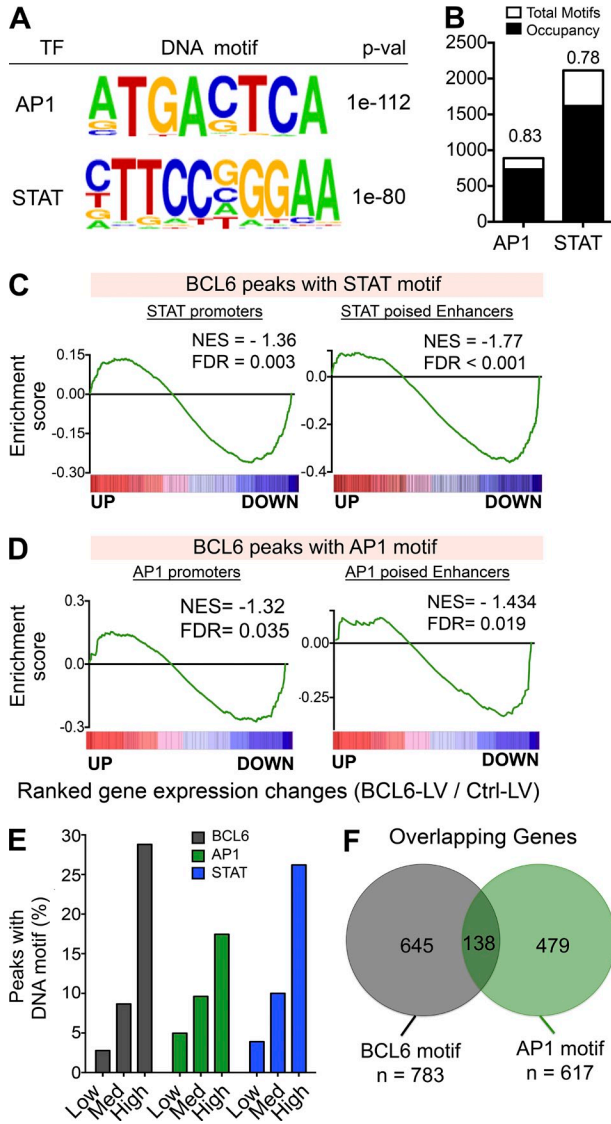


Figure 8. BCL6-mediated repression of key Tfh target genes is linked to interaction with AP1 and recruitment to AP1 DNA-binding sites. (A) De novo motif analysis of BCL6 GC Tfh peaks using HOMER identified the AP1 and STAT DNA motifs among the most highly enriched in Tfh BCL6 peaks. P-values are indicated. (B) Human GC Tfh BCL6-binding sites identified in this study containing AP1 or STAT motifs that were homologous to sites in the mouse genome were queried for AP1 and STAT binding based on published Th17 ChIP-seq datasets. Bound versus unbound fractions are indicated. (C and D) GSEA analysis based on global gene expression changes after BCL6 lentiviral induction in CD4 T cells versus control lentivirus. Up and down indicate the relative gene up- or down-regulation after BCL6 expression. Data are from six independent replicates. The gene sets tested were as follows: (C) promoters with BCL6 peaks containing STAT motifs (left) and poised enhancers with BCL6 peaks containing STAT motifs (right); (D) promoters with BCL6 peaks containing AP1 motifs (left) and poised enhancers with BCL6 peaks containing AP1 motifs (right). FDR is based on 1,000 permutations. (E) Fraction of BCL6 peaks containing BCL6, AP1, or STAT motifs in peaks with lower, intermediate, or high BCL6 enrichment. (F) BCL6 and AP1 motif containing BCL6-bound peaks are primarily found in separate sets of gene.

Harris et al., 1999; Huang et al., 2013). Therefore, a competition between certain STATs and BCL6 in Tfh cells may regulate promoter and enhancer activities, such as the IL17A/F enhancer, which is known to be regulated by competition between STAT3 and STAT5 (Yang et al., 2011).

AP1 factors are transcriptional activators that are crucial in regulating proliferation and cytokine production in T cells and have also been shown to play prominent roles in Th1, Th2, and Th17 cell differentiation (Rincón and Flavell, 1994; Wagner and Eferl, 2005; Schraml et al., 2009). Strikingly, 83% of the 889 BCL6 GC Tfh peaks containing consensus AP1 sites (TGACTCA or TGACGTCA) are occupied by AP1 in activated CD4 T cells (Fig. 8 B). To understand potential mechanistic links between AP1 transcription factors and BCL6 in GC Tfh cells, we first examined how BCL6 affected expression of genes with AP1 motif-associated BCL6 peaks. 454 genes possessed AP1 motif BCL6 promoter peaks, and 177 genes had AP1 motif BCL6 poised enhancer peaks. GSEA analysis found that genes associated with AP1/BCL6 promoters were significantly associated with repression in BCL6⁺ CD4 T cells (FDR = 0.035; Fig. 8 D). GSEA analysis also found that genes associated with AP1/BCL6 poised enhancers were significantly associated with repression in BCL6⁺ CD4 T cells (NES = -1.434, FDR = 0.019; Fig. 8 D). Similar to what we observed for the BCL6 DNA motif, both the AP1 and the STAT consensus DNA motifs occurred more frequently in peaks with the most robust amounts of BCL6 enrichment (Fig. 8 E). Notably, most Tfh BCL6 peaks with AP1 motifs did not contain BCL6 motifs within the same BCL6 peak (742/889; 84%). More specific analysis of promoters and poised enhancers also found that AP1 motif-associated BCL6-bound peaks did not overlap with genes that had BCL6 DNA motif peaks (479/617; 78%; Fig. 8 F). Thus, this results in the interesting conclusion that the BCL6 DNA-binding motif and AP1 DNA-binding motif appear to be largely independent mechanisms used to recruit BCL6 to distinct gene sets.

Collectively, these findings suggest that AP1 motifs are highly associated with repression in the presence of BCL6. AP1 factors may recruit BCL6 to genes, resulting in gene activation being converted to gene repression when BCL6 is present. This could have widespread implications for the functions of BCL6 and AP1 within the cell, given the prominent roles of AP1 in T cell activation. One previous study reported BCL6 could interact with AP1 family members in B cells at *PRDM1* (Vasanwala et al., 2002); however, physical association in cells (coimmunoprecipitation) was not observed, and the overall significance was unclear, with no reported follow up. We therefore first asked whether BCL6 and AP1 factors physically interact in CD4 T cells. To this end, we used a T cell line (MCC) transduced with a BCL6-expressing retroviral vector (BCL6-RV; Fig. 9 A). AP1 immunoprecipitation showed BCL6-AP1 binding in unstimulated Bcl6-RV⁺ cells (Fig. 9 B). Treatment of untransduced MCC cells with PMA and ionomycin induced robust endogenous BCL6 expression (Fig. 9 A). We therefore immunoprecipitated

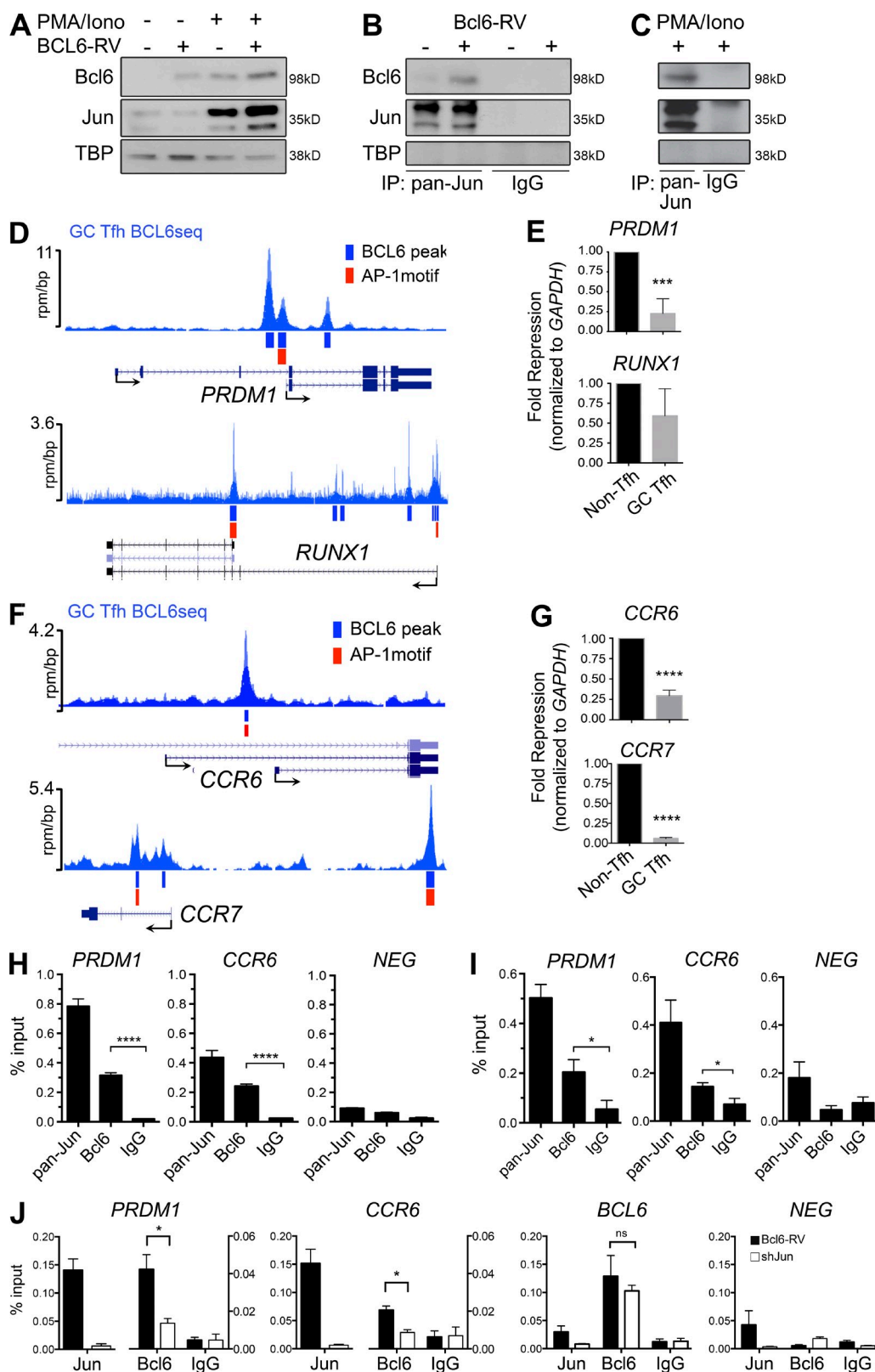


Figure 9. BCL6-mediated repression of key Tfh target genes is linked to interaction with AP1 and recruitment to AP1 DNA-binding sites. (A) Immunoblot of BCL6 and AP1 in MCC cells induced to express BCL6 by retroviral transduction and/or PMA/ionomycin stimulation. (B) Coimmunoprecipitation of BCL6 and AP1 in MCC cells induced to express BCL6 by retroviral transduction. (C) Coimmunoprecipitation of BCL6 and AP1 in MCC cells induced to express BCL6 by PMA/ionomycin stimulation. (A–C) TBP was used as a loading control. Nonspecific IgG served as an immunoprecipitation

AP1 with or without PMA and ionomycin, mimicking TCR stimulation. Endogenous BCL6 was enriched in the AP1 immunoprecipitation from stimulated cells but not in IgG control pulldown or in AP1 pulldown from untreated cells (Fig. 9 C). These results indicate that BCL6 and AP1 physically associate in CD4 T cells, in the presence or absence of TCR stimulation.

Among the AP1 motif-associated BCL6-bound genes in GC Tfh were *PRDM1* and *RUNX1* (promoter BCL6 peaks; Fig. 9 D) and *CCR6* and *CCR7* (enhancer BCL6 peaks; Fig. 9 F). Expression of each of these genes was significantly reduced in GC Tfh cells (Fig. 9, E and G; Rasheed et al., 2006; Ma et al., 2009). To determine whether AP1 is bound at predicted AP1 sites, we performed ChIP experiments for both BCL6 and AP1. Both BCL6 and AP1 were enriched at the *PRDM1* promoter and the *CCR6* enhancer in GC Tfh cells (Fig. 9 H). A negative control locus in *BCL6* intron 9 yielded no enrichment of either protein (Fig. 9 H). To determine whether BCL6 and AP1 are co-recruited at these loci, we performed ChIP-reChIP assays in human tonsillar Tfh cells by immunoprecipitation of AP1 (pan-Jun), followed by immunoprecipitation of BCL6. BCL6 was enriched at both the *PRDM1* and *CCR6* loci (Fig. 9 I), demonstrating co-recruitment of BCL6 and AP1 in vivo.

Finally, to determine whether BCL6 is dependent on AP1 for binding at these loci, we compared BCL6 binding in Bcl6-RV⁺ MCC cells in the presence or absence of cJun knockdown by shRNAmir. The majority of Bcl6 enrichment was lost at AP1 motif-associated Bcl6-bound *PRDM1* and *CCR6* loci after cJun knockdown (Fig. 9 J). As expected, no difference in Bcl6 enrichment was observed at the promoter region of Bcl6, which contains a Bcl6-binding motif and no AP1 motif (Fig. 9 J). Thus, overall, these results suggest that BCL6 is recruited to many genes in Tfh cells in an AP1-specific manner and may either block AP1 activity or serve as a novel AP1/BCL6 repressor complex.

DISCUSSION

In summary, in recent years BCL6 has been identified as a key regulator of Tfh cell differentiation, yet its mechanism of

action in these cells remains largely undiscovered. In this work we identified the genome-wide targets of BCL6 in Tfh cells and the BCL6-regulated Tfh transcriptional program. BCL6 is primarily a repressor in Tfh cells, and it creates a wide umbrella of repression of T cell migration pathways, TCR signaling pathways, and Th1, Th17, Th2, and T reg cell differentiation pathways. Notably, we found that BCL6 is linked to repression of both Tfh promoters and enhancers. Furthermore, it was intriguing to find that BCL6 DNA-binding motifs were only present at ~10% of the bound genes. Given that observation, we then determined that, surprisingly, AP1 motifs were highly enriched within BCL6-bound loci in Tfh cells. Mechanistic experiments showed that BCL6 directly binds AP1 and AP1/BCL6 colocalizes at promoters and enhancers that are repressed by BCL6 in Tfh cells. Altogether, these findings indicate that BCL6 controls Tfh cells via multiple distinct mechanisms, including subversion of AP1. Importantly, this first head-to-head comparison of BCL6 in distinct cell lineages indicates that the BCL6 cistrome is substantially cell context dependent, explaining how this transcription factor can play essential roles in cell types with dramatically different phenotypes. Furthermore, these results provide a foundation for future studies. In particular, studies are warranted to identify the step-wise mechanisms of BCL6-mediated transcriptional repression in these cells, including the corepressor complexes involved in GC Tfh BCL6-mediated transcriptional repression. Because Tfh cells play an essential role in the generation of high-affinity antibody responses and B cell memory, understanding the role of BCL6 in Tfh cell differentiation and homing could help tailor better vaccination strategies (Crotty, 2014) or facilitate the design of targeted therapies for autoimmune disorders (Craft, 2012) or chronic infections (Butler et al., 2012).

MATERIALS AND METHODS

ChIP. GC Tfh cells (CXCR5^{hi} PD1^{hi} CD45RO⁺ CD4⁺ T cells, CD19⁻) were isolated from human tonsils, fixed with 1% formaldehyde, lysed, and sonicated to generate fragments <500 bp. ChIP was performed by incubation of the chromatin with antibodies against BCL6 (N-3; Santa Cruz Biotechnology, Inc.), H3K4me3 (polyclonal rabbit Ab; Abcam), H4K4me1 (polyclonal rabbit Ab; Abcam), and H3K27ac (polyclonal rabbit Ab; Abcam).

negative control. Data shown are representative of five or more experiments. (D) Read density tracks of BCL6 ChIP-seq enrichment in selected GC Tfh cell promoters. (E) Comparison of *PRDM1* and *RUNX1* expression levels in CXCR5⁺ (GC Tfh) versus CXCR5⁻ cells (non-Tfh) calculated by qPCR. (F) GC Tfh BCL6 read density tracks in selected genes with BCL6 peaks at AP1 motif-containing distal and intronic sites. (D and F) BCL6 peaks are indicated in blue and AP1 motifs in red. (G) Comparison of *CCR6* and *CCR7* expression levels in CXCR5⁺ (GC Tfh) versus CXCR5⁻ cells (non-Tfh) calculated by qPCR. (E and G) Fold changes were normalized to GAPDH and are shown relative to non-Tfh. (H) BCL6 and AP1 ChIP performed in human GC Tfh cells (CXCR5^{hi}PD1^{hi}) showing enrichment at the *PRDM1* promoter containing an AP1 motif and the *CCR6* enhancer. Data are from three independent experiments. (I) ChIP-reChIP with AP1 followed by BCL6 performed in human GC Tfh cells (CXCR5^{hi}PD1^{hi}) showing enrichment at the *PRDM1* promoter containing an AP1 motif and the *CCR6* enhancer. Data shown are three technical replicates from each of two independent donors and are representative of three independent experiments. (H and I) Enrichment was calculated as percentage of input chromatin, and nonspecific IgG antibody was used as a negative immunoprecipitation control. BCL6 intron 9 primers were used as a negative control locus. (J) BCL6 and AP1 ChIP performed in Bcl6-RV⁺ MCC cells with and without shRNAmir for cJun showing decreased BCL6 enrichment at the *PRDM1* promoter and the *STAT3* enhancer in treated cells. Enrichment was calculated as percentage of input chromatin, and nonspecific IgG antibody was used as a negative immunoprecipitation control. BCL6 promoter region containing BCL6-binding motif and no AP1 motif was used as a positive control for BCL6 enrichment, and BCL6 intron 9 primers were used as a negative control locus. Data shown are four technical replicates and are representative of three independent experiments. (E and G-J) Error bars indicate SEM. *, P < 0.05; ***, P < 0.001; ****, P < 0.0001.

Immunocomplexes were pulled down using protein A beads, and after increasing stringency washes, 10 ng ChIP DNA was recovered and used to generate a BCL6 ChIP-seq library according to the ChIP-seq Library preparation kit (Illumina). A negative control library was prepared in parallel using 10 ng input chromatin DNA. Libraries were quantified and validated using the 2100 Bioanalyzer (Agilent Technologies) for size, concentration, and purity. Both libraries were sequenced using HiSeq 2000 (Illumina) for 50 cycles.

ChIP-seq data processing and peak detection. Primary image analysis and base calling were conducted using the Illumina pipeline, and the generated reads were mapped to the human genome (UCSC hg18) using ELAND. Only sequences mapped uniquely to the genome with no more than two mismatches were accepted. Read density tracks were visualized using the UCSC browser, and ChIPseeqer algorithm (Giannopoulou and Elemento, 2011) was used for BCL6 peak calling, compared with total input control. Clonal reads (reads mapping to the same exact location) were excluded from peak calling and generation of read density tracks as amplification artifacts. Genomic regions with minimum twofold enrichment over input and negative log p-value >10 were selected. Peaks were then annotated based on the RefSeq database (hg18). Peaks localized ± 2 kb of the TSS were defined as promoter peaks, peaks localized ± 2 kb of the transcriptional end site (TES) were defined as 3' end peaks, and peaks >2 kb away from genes were defined as intergenic (Table S2). De novo transcription factor motif analysis was performed using HOMER (Heinz et al., 2010). Conservation analysis was performed using the ChIPseeqerCons module of ChIPseeqer. Conservation scores centered at each peak summit were computed as the mean placental mammal conservation index (phastCons) extracted from hg18 phastCons44way.placental track of the UCSC Genome Browser database. GC B cell BCL6 ChIP-seq data were from Gene Expression Omnibus (GEO) accession nos. GSE29282 and GSE43350. Gene set enrichment analysis was performed using the GSEA package from the Broad Institute (Subramanian et al., 2007). Statistical analyses were performed using Prism software (Graph-Pad Software) and the R statistical package. Syntenic analysis of BCL6-binding sites and STAT and AP1 motifs in the mouse genome was performed using the Galaxy Lift Over tool (Giardine et al., 2005; Blankenberg et al., 2010; Goecks et al., 2010). AP1- and STAT-binding sites in the mouse genome were identified by Ciofani et al. (2012).

Human samples. Fresh human tonsils were obtained from Rady Children's Hospital of San Diego. Informed consent was obtained from all donors. Tonsils were homogenized using wire mesh and passed through a cell strainer to make a single-cell suspension. Mononuclear cells were isolated using Histopaque 1077 (Sigma Aldrich). All protocols were approved by the La Jolla Institute for Allergy and Immunology, University of California, San Diego, and Rady Children's Hospital of San Diego.

Coimmunoprecipitation assays and Western blot. 10^7 cells were lysed in 1 ml RIPA lysis buffer (150 mM NaCl, 50 mM Tris HCl, 5 mM EDTA, 1% Nonidet P-40, 0.5% sodium deoxycholate, and 0.1% SDS). Cell lysates were kept on ice for 30 min and then centrifuged at 15,000 g at 4°C for 15 min. For coimmunoprecipitation experiments, 250–500 μ g lysates was used diluted in 0.5 ml lysis buffer. Protein G Dynabeads (Life Technologies) were conjugated to 5 μ g each of JunB, JunD (Santa Cruz Biotechnology, Inc.), and cJun (Abcam) or rabbit IgG control (Santa Cruz Biotechnology, Inc.). The cleared lysate was incubated with the conjugated beads overnight at 4°C. The beads were collected by magnetic separation and washed with lysis buffer four times. The beads were mixed with 20 μ l elution buffer and 10 μ l LDS sample buffer with reducing agent (Life Technologies), incubated at 70°C for 10 min, and resolved on a 4–12% (wt/vol) Bis-Tris gel. Western transfer was performed on PVDF membrane, blocked, and incubated with antibodies for pan-Jun (above) and Bcl6 (BD), followed by anti-rabbit IgG peroxidase secondary antibody (Thermo Fisher Scientific) and ECL plus secondary reagent (GE Healthcare).

Cell sorting. All cells were sorted using a FACSAria (BD) as previously described (Kroenke et al., 2012). All Tfh cell sorts were initially gated on CD4⁺CD19⁻, then CD45RO⁺, and then as CXCR5⁻ (non-Tfh) and CXCR5^{hi} (GC Tfh). The following anti-human antibodies were used: CD45RO (clone UCHL1), CD19 (clone HIB19), PD-1 (clone J105), and CD4 (clone RPA-T4; eBioscience); and CXCR5 (clone RF8B2).

shRNAmirs. transOMIC shRNAs are designed using the shERWOOD algorithm, having a proven increasing knockdown potency and specificity at low concentration. cJun shRNAs were cloned into our pLMPd vector as described previously (Chen et al., 2014). Knockdown efficiency was assessed by Western blot. shRNA selected for cJun was transOMIC #RLGM-GU36521 with guide sequence 5'-AGAAACGACCTTCTACGACGAA-3'.

Cell culture and viral transductions. MCC cells were maintained in D10 media (DMEM + 10% FCS supplemented with 2 mM GlutaMAX [Life Technologies] and 100 U/ml penicillin/streptomycin [Life Technologies]). Bcl6-expressing retroviral vector (Bcl6-GFP) or empty vector (GFP only) was used to produce virions from the Plat-E cell line as described previously (Johnston et al., 2009). For shRNA transductions, shcJun-expressing retroviral vector (shcJun-mAmetrine) or negative control vector (shCD8-mAmetrine) was used. Culture supernatants were obtained 2 d after transfections and filtered through 0.45-mm syringe filters. MCC cells were then transduced with retroviral virions two times. Transduced MCC T cells were FACS sorted based on GFP expression levels. For stimulation, cells were treated with 100 ng/ml PMA and 1 μ g/ml ionomycin in D10 media for 5 h. Sorted human tonsil cells were stimulated with anti-CD3/CD28 Dynabeads (Invitrogen) in 96-well flat-bottom plates at a starting density of 7.5×10^4 cells/well. Beads were used at a concentration of 1 ml/well. RPMI 1640 medium with 10% FCS was supplemented with 2 ng/ml recombinant human IL-7. Cells were split as necessary. Sorted naive cells were transduced with lentiviral vectors as previously described (Kroenke et al., 2012).

qPCR. RNA was isolated by RNeasy spin columns (QIAGEN) and reverse transcribed into cDNA using Superscript II reverse transcription (Invitrogen). Real-time PCR reactions were set up using SybrSelect master mix (Life Technologies). Primers are listed in Table S1.

ChIP-qPCR. MCC cells or GC Tfh cells were harvested and then cross-linked with 1% formaldehyde. Chromatin was isolated after sonication. Protein G Dynabeads (Life Technologies) were conjugated to antibodies specific to JunB, JunD, cJun, and Bcl6 (Santa Cruz Biotechnology, Inc.). Rabbit IgG was used as a control. Chromatin was immunoprecipitated using the conjugated beads, eluted, and reverse cross-linked using 0.3 M NaCl at 65°C overnight. qPCR was performed as above, and sample values were given as a percentage of input. Primers are listed in Table S1.

ChIP-reChIP. MCC cells were harvested and then cross-linked with 1% formaldehyde. Chromatin was isolated after sonication. Protein G Dynabeads were conjugated to antibodies specific to cJun (Abcam). Rabbit IgG was used as a control. Chromatin was immunoprecipitated using the cJun-conjugated beads and eluted, followed by immunoprecipitation with Bcl6-conjugated beads. Chromatin was then reverse cross-linked using 0.3 M NaCl at 65°C overnight. qPCR was performed as above, and sample values were calculated as a percentage of input. Primers are listed in Table S1.

Gene expression microarrays. Sorting of tonsil GC Tfh (CXCR5^{hi}PD1^{hi}) cells and Tfh (CXCR5^{int}PD1^{int}) cells was previously described (Kroenke et al., 2012). Microarray method and data were as described previously (Locci et al., 2013). Samples from six independent donors were used. For BCL6-LV microarrays, sorted naive tonsil cells were activated with anti-CD3+CD28 antibody-coated beads and transduced with BCL6 or control lentiviral vectors as described previously (Kroenke et al., 2012). RNA was isolated at day 5 after LV infection, and microarrays were performed as previously described (Locci et al., 2013). Samples from six independent donors were used.

Accession numbers. The human GC Tfh and non-Tfh microarray data are available in the GEO database under the accession no. GSE50391 (ton-sil CD4⁺ T cells). GC Tfh ChIP-seq data are available under accession no. GSE59933. BCL6-LV gene expression microarray has been deposited under GEO accession no. GSE66373.

Online supplemental material. Table S1 lists primers used in the study for qPCR and ChIP assays. Table S2, included as a separate Excel file, shows the peak list. Online supplemental material is available at <http://www.jem.org/cgi/content/full/jem.20141380/DC1>.

We thank Robert Johnston and Michela Locci for experimental assistance early on.

We acknowledge funding from National Institutes of Health (NIH) grants AI109976 and R01 AI072543 (to S. Crotty), National Cancer Institute grant R01 104348 (to A. Melnick), the Burroughs Wellcome Foundation and Chemotherapy Foundation (to A. Melnick), the March of Dimes (to A. Melnick), and NIH grant R01 AI106482 (to E.K. Haddad).

The authors declare no competing financial interests.

Submitted: 22 July 2014

Accepted: 12 March 2015

REFERENCES

- Andersson, R., C. Gebhard, I. Miguel-Escalada, I. Hoof, J. Bornholdt, M. Boyd, Y. Chen, X. Zhao, C. Schmidl, T. Suzuki, et al. FANTOM Consortium. 2014. An atlas of active enhancers across human cell types and tissues. *Nature*. 507:455–461. <http://dx.doi.org/10.1038/nature12787>
- Blankenberg, D., G. Von Kuster, N. Coraor, G. Ananda, R. Lazarus, M. Mangan, A. Nekrutenko, and J. Taylor. 2010. Galaxy: a web-based genome analysis tool for experimentalists. *Curr. Protoc. Mol. Biol.* Chapter 19:1–21. <http://dx.doi.org/10.1002/0471142727.mb1910s89>
- Butler, N.S., J. Moebius, L.L. Pewe, B. Traore, O.K. Doumbo, L.T. Tygrett, T.J. Waldschmidt, P.D. Crompton, and J.T. Harty. 2012. Therapeutic blockade of PD-L1 and LAG-3 rapidly clears established blood-stage *Plasmodium* infection. *Nat. Immunol.* 13:188–195. <http://dx.doi.org/10.1038/ni.2543>
- Carlson, C.M., B.T. Endrizzi, J. Wu, X. Ding, M.A. Weinreich, E.R. Walsh, M.A. Wani, J.B. Lingrel, K.A. Hogquist, and S.C. Jameson. 2006. Kruppel-like factor 2 regulates thymocyte and T-cell migration. *Nature*. 442:299–302. <http://dx.doi.org/10.1038/nature04882>
- Cattoretti, G., C.C. Chang, K. Cechova, J. Zhang, B.H. Ye, B. Falini, D.C. Louie, K. Offit, R.S. Chaganti, and R. Dalla-Favera. 1995. BCL-6 protein is expressed in germinal-center B cells. *Blood*. 86:45–53.
- Chen, R., S. Bélanger, M.A. Frederick, B. Li, R.J. Johnston, N. Xiao, Y.C. Liu, S. Sharma, B. Peters, A. Rao, et al. 2014. In vivo RNA interference screens identify regulators of antiviral CD4⁺ and CD8⁺ T cell differentiation. *Immunity*. 41:325–338. <http://dx.doi.org/10.1016/j.immuni.2014.08.002>
- Choi, Y.S., R. Kageyama, D. Eto, T.C. Escobar, R.J. Johnston, L. Monticelli, C. Lao, and S. Crotty. 2011. ICOS receptor instructs T follicular helper cell versus effector cell differentiation via induction of the transcriptional repressor Bcl6. *Immunity*. 34:932–946. <http://dx.doi.org/10.1016/j.immuni.2011.03.023>
- Ciofani, M., A. Madar, C. Galan, M. Sellars, K. Mace, F. Pauli, A. Agarwal, W. Huang, C.N. Parkurst, M. Muratet, et al. 2012. A validated regulatory network for Th17 cell specification. *Cell*. 151:289–303. <http://dx.doi.org/10.1016/j.cell.2012.09.016>
- Craft, J.E. 2012. Follicular helper T cells in immunity and systemic autoimmunity. *Nat Rev Rheumatol*. 8:337–347. <http://dx.doi.org/10.1038/nrrheum.2012.58>
- Crotty, S. 2014. T follicular helper cell differentiation, function, and roles in disease. *Immunity*. 41:529–542. <http://dx.doi.org/10.1016/j.immuni.2014.10.004>
- Crotty, S. 2015. A brief history of T cell help to B cells. *Nat. Rev. Immunol.* 15:185–189. <http://dx.doi.org/10.1038/nri3803>
- Dent, A.L., A.L. Shaffer, X. Yu, D. Allman, and L.M. Staudt. 1997. Control of inflammation, cytokine expression, and germinal center formation by BCL-6. *Science*. 276:589–592. <http://dx.doi.org/10.1126/science.276.5312.589>
- Gatto, D., D. Paus, A. Basten, C.R. Mackay, and R. Brink. 2009. Guidance of B cells by the orphan G protein-coupled receptor EBI2 shapes humoral immune responses. *Immunity*. 31:259–269. <http://dx.doi.org/10.1016/j.immuni.2009.06.016>
- Giannopoulou, E.G., and O. Elemento. 2011. An integrated ChIP-seq analysis platform with customizable workflows. *BMC Bioinformatics*. 12:277. <http://dx.doi.org/10.1186/1471-2105-12-277>
- Giardine, B., C. Riemer, R.C. Hardison, R. Burhans, L. Elnitski, P. Shah, Y. Zhang, D. Blankenberg, I. Albert, J. Taylor, et al. 2005. Galaxy: a platform for interactive large-scale genome analysis. *Genome Res*. 15:1451–1455. <http://dx.doi.org/10.1101/gr.4086505>
- Goecks, J., A. Nekrutenko, and J. Taylor. Galaxy Team. 2010. Galaxy: a comprehensive approach for supporting accessible, reproducible, and transparent computational research in the life sciences. *Genome Biol.* 11:R86. <http://dx.doi.org/10.1186/gb-2010-11-8-r86>
- Harris, M.B., C.C. Chang, M.T. Berton, N.N. Daniai, J. Zhang, D. Kuehner, B.H. Ye, M. Kvatyuk, P.P. Pandolfi, G. Cattoretti, et al. 1999. Transcriptional repression of Stat6-dependent interleukin-4-induced genes by BCL-6: specific regulation of I ϵ transcription and immunoglobulin E switching. *Mol. Cell Biol.* 19:7264–7275.
- Hatzi, K., and A. Melnick. 2014. Breaking bad in the germinal center: how deregulation of BCL6 contributes to lymphomagenesis. *Trends Mol. Med.* 20:343–352. <http://dx.doi.org/10.1016/j.molmed.2014.03.001>
- Heinz, S., C. Benner, N. Spann, E. Bertolino, Y.C. Lin, P. Laslo, J.X. Cheng, C. Murre, H. Singh, and C.K. Glass. 2010. Simple combinations of lineage-determining transcription factors prime cis-regulatory elements required for macrophage and B cell identities. *Mol. Cell*. 38:576–589. <http://dx.doi.org/10.1016/j.molcel.2010.05.004>
- Huang, C., K. Hatzi, and A. Melnick. 2013. Lineage-specific functions of Bcl-6 in immunity and inflammation are mediated by distinct biochemical mechanisms. *Nat. Immunol.* 14:380–388. <http://dx.doi.org/10.1038/ni.2543>
- Huang, C., D.G. Gonzalez, C.M. Cote, Y. Jiang, K. Hatzi, M. Teater, K. Dai, T. Hla, A.M. Haberman, and A. Melnick. 2014. The BCL6 RD2 domain governs commitment of activated B cells to form germinal centers. *Cell Reports*. 8:1497–1508. <http://dx.doi.org/10.1016/j.celrep.2014.07.059>
- Johnston, R.J., A.C. Poholek, D. DiToro, I. Yusuf, D. Eto, B. Barnett, A.L. Dent, J. Craft, and S. Crotty. 2009. Bcl6 and Blimp-1 are reciprocal and antagonistic regulators of T follicular helper cell differentiation. *Science*. 325:1006–1010. <http://dx.doi.org/10.1126/science.1175870>
- Kroenke, M.A., D. Eto, M. Locci, M. Cho, T. Davidson, E.K. Haddad, and S. Crotty. 2012. Bcl6 and Maf cooperate to instruct human follicular helper CD4 T cell differentiation. *J. Immunol.* 188:3734–3744. <http://dx.doi.org/10.4049/jimmunol.1103246>
- Kusam, S., L.M. Toney, H. Sato, and A.L. Dent. 2003. Inhibition of Th2 differentiation and GATA-3 expression by BCL-6. *J. Immunol.* 170:2435–2441. <http://dx.doi.org/10.4049/jimmunol.170.5.2435>
- Lee, J.-Y., C.N. Skon, Y.J. Lee, S. Oh, J.J. Taylor, D. Malhotra, M.K. Jenkins, M.G. Rosenfeld, K.A. Hogquist, and S.C. Jameson. 2015. The transcription factor KLF2 restrains CD4⁺ T follicular helper cell differentiation. *Immunity*. 42:252–264. <http://dx.doi.org/10.1016/j.immuni.2015.01.013>
- Liu, X., X. Chen, B. Zhong, A. Wang, X. Wang, F. Chu, R.I. Nurieva, X. Yan, P. Chen, L.G. van der Flier, et al. 2014. Transcription factor achaete-scute homologue 2 initiates follicular T-helper-cell development. *Nature*. 507:513–518. <http://dx.doi.org/10.1038/nature12910>
- Locci, M., C. Havenar-Daughton, E. Landais, J. Wu, M.A. Kroenke, C.L. Arlehamn, L.F. Su, R. Cubas, M.M. Davis, A. Sette, et al. International AIDS Vaccine Initiative Protocol C Principal Investigators. 2013. Human circulating PD-1⁺CXCR3⁻CXCR5⁺ memory Tfh cells are highly functional and correlate with broadly neutralizing HIV antibody responses. *Immunity*. 39:758–769. <http://dx.doi.org/10.1016/j.immuni.2013.08.031>
- Ma, C.S., S. Suryani, D.T. Avery, A. Chan, R. Nanan, B. Santner-Nanan, E.K. Deenick, and S.G. Tangye. 2009. Early commitment of naïve human CD4⁺ T cells to the T follicular helper (T_{FH}) cell lineage is induced by IL-12. *Immunol. Cell Biol.* 87:590–600. <http://dx.doi.org/10.1038/icb.2009.64>

- Nurieva, R.I., Y. Chung, G.J. Martinez, X.O. Yang, S. Tanaka, T.D. Matskevitch, Y.H. Wang, and C. Dong. 2009. Bcl6 mediates the development of T follicular helper cells. *Science*. 325:1001–1005. <http://dx.doi.org/10.1126/science.1176676>
- Pereira, J.P., L.M. Kelly, Y. Xu, and J.G. Cyster. 2009. EB12 mediates B cell segregation between the outer and centre follicle. *Nature*. 460: 1122–1126.
- Poholek, A.C., K. Hansen, S.G. Hernandez, D. Eto, A. Chandele, J.S. Weinstein, X. Dong, J.M. Odegard, S.M. Kaech, A.L. Dent, et al. 2010. In vivo regulation of Bcl6 and T follicular helper cell development. *J. Immunol.* 185:313–326. <http://dx.doi.org/10.4049/jimmunol.0904023>
- Rasheed, A.U., H.P. Rahn, F. Sallusto, M. Lipp, and G. Müller. 2006. Follicular B helper T cell activity is confined to CXCR5^{hi}ICOS^{hi} CD4 T cells and is independent of CD57 expression. *Eur. J. Immunol.* 36: 1892–1903. <http://dx.doi.org/10.1002/eji.200636136>
- Rincón, M., and R.A. Flavell. 1994. AP-1 transcriptional activity requires both T-cell receptor-mediated and co-stimulatory signals in primary T lymphocytes. *EMBO J.* 13:4370–4381.
- Schraml, B.U., K. Hildner, W. Ise, W.L. Lee, W.A. Smith, B. Solomon, G. Sahota, J. Sim, R. Mukasa, S. Cemerski, et al. 2009. The AP-1 transcription factor Batf controls T_H17 differentiation. *Nature*. 460:405–409. <http://dx.doi.org/10.1038/nature08114>
- Shaffer, A.L., X. Yu, Y. He, J. Boldrick, E.P. Chan, and L.M. Staudt. 2000. BCL-6 represses genes that function in lymphocyte differentiation, inflammation, and cell cycle control. *Immunity*. 13:199–212. [http://dx.doi.org/10.1016/S1074-7613\(00\)00020-0](http://dx.doi.org/10.1016/S1074-7613(00)00020-0)
- Stone, E.L., M. Pepper, C.D. Katayama, Y.M. Kerdiles, C.-Y. Lai, E. Emslie, Y.C. Lin, E. Yang, A.W. Goldrath, M.O. Li, et al. 2015. ICOS coreceptor signaling inactivates the transcription factor FOXO1 to promote Tfh cell differentiation. *Immunity*. 42:239–251. <http://dx.doi.org/10.1016/j.immuni.2015.01.017>
- Subramanian, A., H. Kuehn, J. Gould, P. Tamayo, and J.P. Mesirov. 2007. GSEA-P: a desktop application for Gene Set Enrichment Analysis. *Bioinformatics*. 23:3251–3253. <http://dx.doi.org/10.1093/bioinformatics/btm369>
- Tunayaplin, C., A.L. Shaffer, C.D. Angelin-Duclos, X. Yu, L.M. Staudt, and K.L. Calame. 2004. Direct repression of prdm1 by Bcl-6 inhibits plasmacytic differentiation. *J. Immunol.* 173:1158–1165. <http://dx.doi.org/10.4049/jimmunol.173.2.1158>
- Vahedi, G., H. Takahashi, S. Nakayamada, H.W. Sun, V. Sartorelli, Y. Kanno, and J.J. O’Shea. 2012. STATs shape the active enhancer landscape of T cell populations. *Cell*. 151:981–993. <http://dx.doi.org/10.1016/j.cell.2012.09.044>
- Vasanwala, F.H., S. Kusam, L.M. Toney, and A.L. Dent. 2002. Repression of AP-1 function: a mechanism for the regulation of Blimp-1 expression and B lymphocyte differentiation by the B cell lymphoma-6 proto-oncogene. *J. Immunol.* 169:1922–1929. <http://dx.doi.org/10.4049/jimmunol.169.4.1922>
- Wagner, E.F., and R. Eferl. 2005. Fos/AP-1 proteins in bone and the immune system. *Immunol. Rev.* 208:126–140. <http://dx.doi.org/10.1111/j.0105-2896.2005.00332.x>
- Weber, J.P., F. Fuhrmann, R.K. Feist, A. Lahmann, M.S. Al Baz, L.J. Gentz, D. Vu Van, H.W. Mages, C. Haftmann, R. Riedel, et al. 2015. ICOS maintains the T follicular helper cell phenotype by down-regulating Krüppel-like factor 2. *J. Exp. Med.* 212:217–233. <http://dx.doi.org/10.1084/jem.20141432>
- Weinstein, J.S., K. Lezon-Geyda, Y. Maksimova, S. Craft, Y. Zhang, M. Su, V.P. Schulz, J. Craft, and P.G. Gallagher. 2014. Global transcriptome analysis and enhancer landscape of human primary T follicular helper and T effector lymphocytes. *Blood*. 124:3719–3729. <http://dx.doi.org/10.1182/blood-2014-06-582700>
- Xiao, N., D. Eto, C. Elly, G. Peng, S. Crotty, and Y.-C. Liu. 2014. The E3 ubiquitin ligase Itch is required for the differentiation of follicular helper T cells. *Nat. Immunol.* 15:657–666. <http://dx.doi.org/10.1038/ni.2912>
- Yang, X.O., B.P. Pappu, R. Nurieva, A. Akimzhanov, H.S. Kang, Y. Chung, L. Ma, B. Shah, A.D. Panopoulos, K.S. Schluns, et al. 2008. T helper 17 lineage differentiation is programmed by orphan nuclear receptors ROR α and ROR γ . *Immunity*. 28:29–39. <http://dx.doi.org/10.1016/j.immuni.2007.11.016>
- Yang, X.P., K. Ghoreschi, S.M. Steward-Tharp, J. Rodriguez-Canales, J. Zhu, J.R. Grainger, K. Hirahara, H.W. Sun, L. Wei, G. Vahedi, et al. 2011. Opposing regulation of the locus encoding IL-17 through direct, reciprocal actions of STAT3 and STAT5. *Nat. Immunol.* 12:247–254. <http://dx.doi.org/10.1038/ni.1995>
- Yu, D., S. Rao, L.M. Tsai, S.K. Lee, Y. He, E.L. Sutcliffe, M. Srivastava, M. Linterman, L. Zheng, N. Simpson, et al. 2009. The transcriptional repressor Bcl-6 directs T follicular helper cell lineage commitment. *Immunity*. 31:457–468. <http://dx.doi.org/10.1016/j.immuni.2009.07.002>